Control Engineering Practice 92 (2019) 104072

Contents lists available at ScienceDirect

Control Engineering Practice

journal homepage: www.elsevier.com/locate/conengprac

Brake and velocity model-free control on an actual vehicle

Philip Polack [a,*], Sébastien Delprat [b], Brigitte d'Andréa-Novel [c,1]

[a] MINES ParisTech, PSL Research University, Center of Robotics, 60 boulevard Saint-Michel, 75006 Paris, France
[b] Univ. Valenciennes, CNRS, UMR 8201 - LAMIH Laboratoire d'Automatique de Mécanique et d'Informatique Industrielles et Humaines, ENSIAME École nationale supérieure d'ingénieurs en informatique, automatique, mécanique, énergétique et électronique, F-59313 Valenciennes, France
[c] IRCAM, CNRS-UMR9912-STMS, Sorbonne Université, 1 place Igor Stravinsky, 75004 Paris, France

ARTICLE INFO

Keywords:
Model-free control
Intelligent controllers
Longitudinal control
Tuning procedure
ALIEN filters

ABSTRACT

A tuning procedure for the model-free control paradigm introduced in Fliess and Join (2013) is proposed. This controller requires an estimate of the system dynamics usually obtained using an ALIEN filter, presented in Fliess and Sira-Ramírez (2003). Several implementation issues of this ALIEN filter, such as the order of the numerical quadrature, are discussed and overcome. Finally, the control law is applied to two systems: the low-level braking system of a vehicle and its longitudinal speed control. Experimental results on a real vehicle are provided and compared with a classic PI controller.

1. Introduction

Using model-free control can be a risky project since the closed-loop stability can hardly be proven in general. However, it remains an appealing solution when a model is not available due to the system complexity or to its development cost (engineering time and/or required hardware). Proportional–Integral–Derivative (PID) controllers (see Åstrom & Hägglund, 1995) are among the most popular model-free controllers in industrial applications due to their limited number of parameters and quite intuitive tuning for a large class of systems (IFAC Industry Committee, 2015). The model-free control (MFC) approach introduced by Fliess and Join (2013) extends the classic PID framework and provides "*intelligent*"-PID controllers allowing to account for the unknown dynamics of the system. Hence, the considered MFC structure provides a model-free feedforward control that can be used to improve the reference tracking. It is also able to handle some complex non-linear control problems (Fliess & Join, 2009) at a low computational cost as these control laws can be implemented on cheap and small programmable devices (Join, Chaxel, & Fliess, 2013). Finally, as model-free control does not depend on a nominal model, it can be seen as an implicitly robust control framework. It has been successfully applied among others to energy management in buildings supplied by solar photovoltaic panels (Bara et al., 2017) and to flapping wings (Chand, Kawanishi, & Narikiyo, 2016). Note that there exists a wide literature about other model-free data-based control techniques, such as model-free adaptive control (Hou & Jin, 2013), virtual reference feedback tuning (Campi, Lecchini, & Savaresi, 2002; Guardabassi & Savaresi, 2000), direct and indirect model reference adaptive control (Narendra & Valavani, 1979), iterative feedback tuning (Hjalmarsson, Gevers, Gunnarsson, & Lequin, 1998), fuzzy control (Zimmermann, 1996) and neural-network based control methods (Miller, Werbos, & Sutton, 1995). See also Hou and Wang (2013) for a review of existing data-driven control approaches.

In this work, the brake and engine coordinated longitudinal control of a vehicle is addressed. MFC framework is especially relevant in that case since the dynamics of the low-level actuators are complex and unknown. On the one hand, the vehicle propelling is ensured by an internal combustion engine (ICE) controlled by the original engine control unit (ECU) of the vehicle. On the other hand, the mechanical brakes are actuated using a hydraulic actuator connected to the brake pedal. Therefore, the low-level dynamics is highly complex. Moreover, the brake and throttle dynamics are very different between them.

Existing work on MFC applied to the longitudinal dynamics of a vehicle includes:

(i) simulation results based on actual driver data (d'Andréa-Novel, 2018; d'Andréa-Novel, Menhour, Fliess, & Mounier, 2016; Menhour, d'Andréa-Novel, Fliess, Gruyer, & Mounier, 2015; Menhour, d'Andréa-Novel, Fliess, & Mounier, 2013);
(ii) a combination with event-triggered control (Wang, Mounier, Cela, & Niculescu, 2011);
(iii) a combination with Stop-and-Go strategies (Choi, d'Andréa-Novel, Fliess, Mounier, & Villagra, 2009; Milanés, Villagrá, Godoy and González, 2012; Villagra, Milanes, Perez, & Gonzalez, 2010).

* Corresponding author.
E-mail addresses: philip.polack@mines-paris.org (P. Polack), sebastien.delprat@univ-valenciennes.fr (S. Delprat), brigitte.dandrea-novel@mines-paristech.fr (B. d'Andréa-Novel).
[1] Brigitte d'Andréa-Novel is also with MINES ParisTech, PSL Research University, Center of Robotics, 60 boulevard Saint-Michel, 75006 Paris, France.

https://doi.org/10.1016/j.conengprac.2019.06.011
Received 16 April 2018; Received in revised form 8 April 2019; Accepted 15 June 2019
Available online xxxx
0967-0661/

Fig. 1. The experimental vehicle.

Reference Join, Masse, and Fliess (2008) which applies MFC for controlling the throttle of an engine can also be mentioned. To the best of the authors' knowledge, only (Milanés, Villagrá, Godoy et al., 2012; Milanés, Villagrá, Perez and González, 2012) tested on an actual vehicle the coordinated control of both actuators within a MFC framework. The authors compared MFC, PID and fuzzy control for: (i) controlling the longitudinal lower-level of a Stop-and-Go controller (Milanés, Villagrá, Godoy et al., 2012); (ii) for longitudinal control at very low speed (Milanés, Villagrá,Perez et al., 2012). More precisely, they account for the use of two different MFC laws working alternatively: one for the throttle and one for the brake.

In the present work, a cascading structure is suggested. At the high-level, the MFC computes the total force to be applied to the chassis, which is split between the two different low-level controllers. At the low-level, another MFC deals with the unknown dynamics of the braking circuit whereas the engine control unit (ECU) remains in charge of the engine torque production.

Compared to Milanés, Villagrá, Godoy et al. (2012), this work relies on ALIEN filters introduced in Fliess and Sira-Ramírez (2003) to estimate the vehicle dynamics in order to be robust to noise measurements. Moreover, only the intelligent-Proportional (i-P) controller is investigated and a methodology for the tuning of the control parameters is also proposed.

The purpose of this work is then to discuss an effective way to implement these MFC laws on an actual vehicle. The main contributions are the numerical implementation of the ALIEN filters and the tuning procedure of the model-free controllers.

The rest of the paper is then organized as follows: first, in Section 2, the theoretical working principle of model-free control is recalled; then, Section 3 discusses the practical implementation details mentioned in the previous paragraph. In particular, a simple and efficient tuning procedure that can be applied on an actual system without any prior simulation results is introduced. The application to an internal combustion engine vehicle, shown in Fig. 1, is presented in Section 4 and experimental results are discussed. Finally, Section 5 concludes this work.

2. The model-free control paradigm

2.1. The ultralocal model

The principle of the model-free control paradigm introduced in Fliess and Join (2013) is to replace a complex nonlinear model by an ultralocal model given by (see Appendix A for more details):

$$y^{(\nu)}(t) = F(t) + \alpha u(t) \tag{1}$$

u is the control input, y is the observed output, ν is the order of the system, F represents both the unmodeled dynamics and the disturbances and α is a constant parameter chosen by the practitioner. In the rest of this work, $\nu = 1$ has been chosen by the practitioner. When there is no ambiguity, the time dependency will be omitted. Furthermore, the sign of α should match the sign of the actual system input gain. In the studied framework, α being a constant, systems with a time varying input gain that takes values in both $\mathbb{R}^+$ and $\mathbb{R}^-$ are not considered.

2.2. Estimation of $\widehat{F}$

At each time step $t_k = kT_s$ where T_s is the sampling time step of the measurements, the dynamic F is estimated from the previous control inputs u applied to the system and outputs y observed. The estimation of F at time t, denoted $\widehat{F}$, is assumed to remain constant over $[t; t+T]$. Therefore, using the model-free control approach requires to have a high measurement frequency compared to the time constant of the system one wants to control. A direct method for estimating $\widehat{F}_k$ at time t_k is given by:

$$\widehat{F}_k = \dot{y}_k - \alpha u_{k-1} \tag{2}$$

However, measurements are usually noisy. Therefore, using a filter is highly recommended. In the rest of the present communication, ALIEN[2] filters introduced by Fliess and Sira-Ramírez (2003) are used. For a first-order ultralocal model, one obtains Eq. (3), where T denotes the time window of the filter. The computation details can be found in Appendix B.

$$\widehat{F}_k = -\frac{6}{T^3}\int_{t_k-T}^{t_k} [(T-2\tau)y(\tau) + \alpha\tau(T-\tau)u(\tau)]\,\mathrm{d}\tau \tag{3}$$

2.3. Intelligent-PID controllers

The "intelligent" controllers have been introduced within the model-free control paradigm (Fliess & Join, 2008). For a first-order system, an intelligent-Proportional–Integral (i-PI) or an intelligent-Proportional (i-P) controller given by Eq. (4) and completed respectively by Eqs. (5) and (6) can be used:

$$u = -\frac{\widehat{F} - \dot{y}_r}{\alpha} - \mathcal{K}(e) \tag{4}$$

$$(i-PI) \qquad \mathcal{K}(e) = K_P e + K_I \int_0^t e\,d\tau \tag{5}$$

$$(i-P) \qquad \mathcal{K}(e) = K_P e \tag{6}$$

where $e = y - y_r$ is the tracking error. K_P and K_I denote respectively the proportional and the integral gains. Note that the reference y_r must be a C^1 signal. This can be enforced, for instance, using a first-order linear low-pass filter on the original reference signal.

Combining Eqs. (1) and (4) for $\nu = 1$ leads to the following equation for the tracking error e:

$$\dot{e}(t) = -\alpha\mathcal{K}(e(t)) + (F(t) - \widehat{F}(t)) \tag{7}$$

Therefore, if the estimation of $\widehat{F}$ is "good", *i.e.* $(F - \widehat{F}) \approx 0$, "intelligent" controllers ensure the asymptotic stability of the closed-loop system. In particular, an i-P controller is sufficient for $\alpha > 0$ and $K_p > 0$ as the evolution of the tracking error e is ruled by:

$$\dot{e}(t) = -\alpha K_P e(t) \tag{8}$$

Thus in practice, the core of the i-P controller is the estimation of the unknown signal F. It can be derived, as in d'Andréa-Novel, Fliess, Join, Mounier, and Steux (2010), using a first order discretization of the output signal (in Eq. (2)) and its derivative. In that case, the structure of the i-P controller is equivalent to a PI controller. Therefore the

[2] ALgebra for Numerical Identification and Estimation.

benefits of the i-P structure compared to a classic PI comes from a good estimation of the unknown signal F. Hence the discretization of the ALIEN filter needs to be studied carefully. Moreover, the structure allows performing a feedforward control without explicitly needing a model (although it requires a good estimation of the unknown signal F).

Remark 1. Under the assumption that the ∞-norm of the estimation error $\|F-\hat{F}\|_\infty$ is bounded (which is weaker than the perfect estimation assumption widely encountered in the literature), it is still possible to prove the stability (convergence in a ball centered in 0) as shown in Appendix C.

3. Applying model-free control on an actual system

In order to apply the model-free control paradigm on an actual system, it is necessary to have a good estimation of the unknown signal F. For that purpose, two main difficulties need to be overcome. First, the numerical implementation of the ALIEN filter is not straightforward but it is crucial if one wants to achieve good performances in particular at steady-state. This will be discussed in Section 3.1. Secondly, the performances of model-free control laws are highly influenced by the value of parameter α, in particular during transient phases. Therefore, a tuning procedure is proposed in Section 3.2.

3.1. Numerical implementation of ALIEN filters

One of the main difficulty for applying the MFC paradigm defined previously on an actual system is to compute numerically the ALIEN filter given by Eq. (3). First of all, it is important to provide the actual control u that was applied on the system, and not the one send by the controller as they might differ due to filters or limitations on the actuators.

Theorem 1. *In order to have a perfect estimation of F at steady-state, the numerical quadrature to compute Eq. (3) should be at least of order 2.*

Proof. Assume that the system has reached its steady state, denoted by the subscript ∞. In this case, Eq. (1) becomes:

$$F_\infty = -\alpha u_\infty \tag{9}$$

and the expression of the ALIEN filter given by Eq. (3) becomes:

$$\hat{F}_\infty = -\frac{6}{T^3}\int_{t-T}^{t} P_2(\tau)\,\mathrm{d}\tau \tag{10}$$

where $P_2(\tau) = Ty_\infty + (-2y_\infty + \alpha T u_\infty)\tau - \alpha u_\infty \tau^2$ is a second order polynomial in τ.

The *order of accuracy* n of a quadrature rule is defined as the biggest integer value such that the numerical approximation is correct for any polynomial of degree less or equal to n (Dahlquist & Björck, 2008), which concludes the proof. □

Thus, a classic numerical approximation such as the trapezoidal rule which is of order 1 is not sufficient: in that case the estimation error $F-\hat{F}$ is equal to $+\frac{1}{2}\left(\frac{T_s}{T}\right)^2 F$ (see Appendix D). However choosing $T \gg T_s$ enables to improve the accuracy in this particular case.

Therefore, Eq. (3) should be approximated using one of the two Simpson's rules given by Eqs. (11) and (12), which are both of order 3:

- Simpson's 1/3 rule (or three-point Newton–Cotes quadrature rule)

$$\int_a^b f(x)dx \approx \frac{b-a}{6}\left(f(a)+4f\left(\frac{a+b}{2}\right)+f(b)\right) \tag{11}$$

- Simpson's 3/8 rule (or four-point Newton–Cotes quadrature rule)

$$\int_a^b f(x)dx \approx \frac{b-a}{8}\left(f(a)+3f\left(\frac{a+b}{3}\right)+3f\left(\frac{2(a+b)}{3}\right)+f(b)\right) \tag{12}$$

Newton–Cotes formulas generalize the Simpson rule for interpolation with arbitrary degree polynomials. However, in practice, using high-degree polynomials for interpolation can lead to instability. This is referred as Runge's phenomenon (Schlömilch et al., 1901). Therefore, cutting the computation of the integral into subdivisions is recommended.

In the rest of this work, the time window $T = 2kT_s$ (with $k \in \mathbb{N}^*$) of the ALIEN filter is chosen such that $[0, T]$ can be subdivided into subsegments where the rule given by Eq. (11) can be applied.

3.2. Tuning procedure

In this subsection, a tuning procedure for the parameter α will be presented as it also plays an important role in limiting the estimation error, in particular during the transient phases.

Write the actual output signal dynamics as following where $\overline{F}(t)$ and $\overline{\alpha}(t)$ are two unknown functions of time:

$$\dot{y} = \overline{F}(t) + \overline{\alpha}(t)u \tag{13}$$

In that case:

$$F = \overline{F}(t) + (\overline{\alpha}(t) - \alpha)u \tag{14}$$

$$u = -\left(\frac{\hat{F}-\dot{y}_r}{\alpha}\right) - \mathcal{K}(e) \tag{15}$$

where $\mathcal{K}(e)$ is the correction on the tracking error. Combining Eq. (13) with (15) and choosing $\mathcal{K}(e) = 0$, *i.e.* considering only the feedforward term of the control law, leads to:

$$\dot{y} = \frac{\overline{\alpha}(t)}{\alpha}\dot{y}_r + \left(\overline{F}(t) - \frac{\overline{\alpha}(t)}{\alpha}\hat{F}\right) \tag{16}$$

Assuming a perfect estimation of F, *i.e.* $\hat{F} = F$, Eqs. (14) and (16) become Eq. (17). Therefore, in theory, any value of α should work. Nevertheless, if $\hat{F} = F$, the solution of Eqs. (1) and (4) is independent of the control: the control u cannot be computed anymore.

$$\dot{y} = \dot{y}_r \tag{17}$$

However, in practice, the estimation $\hat{F}$ is subject to some dynamics, and the closed-loop cannot be reduced to Eq. (17). As the quality of the controller depends mostly on the estimation error $(F-\hat{F})$, the value of α needs to be chosen carefully, as close to the real gain of the system, to avoid big variations of F.

If $\alpha \to +\infty$, the control u given by Eq. (15) is reduced to $\mathcal{K}(e)$. In other words, the controller is reduced to a classic proportional one.

If $\alpha \to 0^+$, the control u depends mostly on the estimation $\hat{F}$. As F depends on u, the behavior of the closed-loop mostly depends both on the unknown system dynamics and the ALIEN filter dynamics. The resulting dynamics is quite unpredictable and this situation should be avoided.

It should be noticed that when α is close to the input gain $\overline{F}(t)$, F is almost independent of u and its estimation becomes easier in practice, leading to a smaller estimation error.

Therefore, tuning α becomes quite straightforward for a stable open-loop system: the practitioner should set $\mathcal{K}(e) = 0$ and observe, for different values of α, the response of the system to the control law:

$$u = -\left(\frac{\hat{F}-\dot{y}_r}{\alpha}\right) \tag{18}$$

Starting with an α large enough, the control will be almost zero. Then, decreasing the value of α will increase the control value until

Table 1
Model-free controller tuning guidelines.

Initialization:
Set $\mathcal{K}(e) = 0$;
Choose α large enough;
Feedforward tuning
Rule n°1: run the experiment; while the average value of $\lvert\dot{y} - \dot{y}_r\rvert$ decreases, decrease α and repeat rule n°1;
Rule n°2: if the system output oscillates around the setpoint, increase α;
Feedback tuning
Rule n°1: increase K_p progressively until (i) tracking error $\lvert y - y_r\rvert$ is low and (ii) disturbances are rejected.

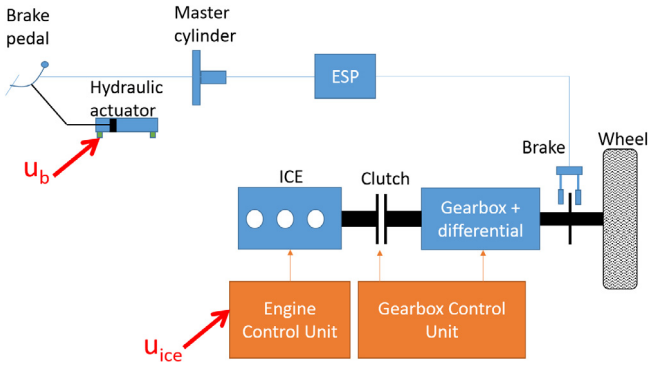

Fig. 2. Structure of the vehicle powertrain to be controlled.

the desired closed-loop response given by Eq. (17) is achieved. If α is decreased too much, the control amplitude will become too high and the system may oscillate. The tuning guidelines of α are summarized in Table 1.

Once α has been chosen correctly, the gains of $\mathcal{K}(e)$ have to be tuned. It can be noticed that the feedforward control only ensures a good tracking of the reference derivative. $\mathcal{K}(e)$ is used to track the reference and its tuning is similar to the one of classic P and PI controllers. In practice, an i-P controller is usually sufficient. The disturbances are implicitly embedded within the unknown term F in the model given by Eq. (1) and are therefore estimated by the ALIEN filter. Thus, they are rejected by the control law of Eq. (18). The correcting term $\mathcal{K}(e)$ is mostly used to overcome the error due to initial conditions and estimation errors of F due to the dynamics of the filter.

4. Application to the longitudinal control of an actual vehicle: experimental results

The longitudinal control of a vehicle is used as an illustration of the proposed method. The structure of the vehicle prototype used for the experiment is depicted in Fig. 2. All the sensors and actuators are connected to the CAN bus and work with a fixed sampling period of 10 ms. The vehicle velocity is provided by the original sensor of the vehicle located on the gearbox output shaft. The propelling is ensured by the torque produced by the engine which is controlled by the Engine Control Unit (ECU). The ICE torque, which dynamics is unknown, is transmitted to the wheels through the clutch and the gearbox which are controlled by the Gearbox Control Unit (GCU). This unit is independent and operates using its own unknown rules. The braking circuit comprises the brake pedal, the master cylinder, the Electronic Stability Program (ESP) block and the mechanical brakes. The brake pedal is actuated using an hydraulic cylinder. Two control inputs are available to control the vehicle velocity: u_b that controls the hydraulic cylinder pressures of the brakes and u_{ice} the ICE torque setpoint.

Therefore, the considered control structure, see Fig. 3, comprises two parts. First, a high-level velocity controller computes the total force

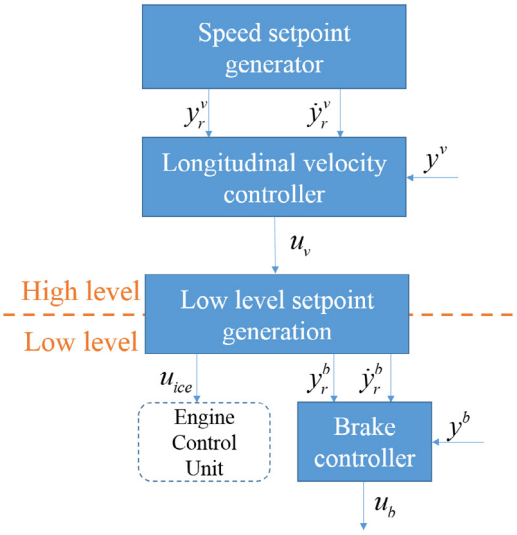

Fig. 3. Considered cascading control structure.

u_v to be generated by both the brakes and the engine according to the actual vehicle velocity y^v and the reference velocity y_r^v and acceleration $\dot{y}_r^v$. According to the braking capability of the ICE (estimated by the ECU), this high-level control signal is then split into two signals: u_{ice}, the ICE torque setpoint, which is sent to the original vehicle ECU, and y_b^r, the brake pedal position setpoint, which is sent to the brake model-free controller only when ICE-based braking is not enough to reach the total force u_v. A static map is used to approximately convert the braking force into brake pedal position. In practice, the actual braking force differs significantly from the static map data due to thermal effect, unknown dynamics of the master cylinder and hydraulic braking system.

4.1. Brake control

The brake system consists of an hydraulic actuator that pushes or pulls the brake pedal. The position of the latter determines the pressure generated by the master cylinder on the brake disk. The master cylinder and the brake pedal are connected together through a pushrod subject to some stiction which makes the system very difficult to model. Also, the brake pedal dynamics is non-linear due to the master cylinder's resistive force. The objective is to control the brake pedal position y^b by opening the valves ($u_b \in [-80; 80]\%$) located respectively at the top and at the bottom of the hydraulic actuator. The system is described in Fig. 4. The main difficulties to control such a system are: (i) the possible occurrence of limit cycles due to pushrod stiction; (ii) reduced stability margin due to communication delays; (iii) variations of the system gain due to the return spring and the internal pressure of the master cylinder; (iv) unpredictable variations of the system gain over time due to the pressure of the tank and the pump. Note that the system is subject to a known 20 ms communication delay. The so-called "position" signal is generated by a control unit on the CAN bus. When the brake pedal is fully released, the "position" signal is 700; when it is fully pressed, the signal is 1600.

The open-loop response of the system to different input steps is depicted in Fig. 5 and illustrates the non-linear behavior of the system. The cumulated effect of stiction and communication delays induces a response "delay" between 60 ms and 180 ms.

The MFC law was applied using the tuning method suggested in Section 3.2 while the vehicle is at standstill with the engine turned on. The overall tuning takes only a few minutes. First, the proportional gain K_P is set to 0. The system being at the rest position, a reference signal is generated and the open-loop responses are recorded for different values

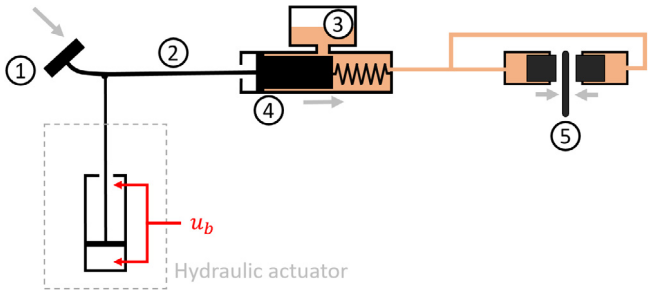

Fig. 4. Description of the brake system: the brake pedal (1) pushes the master cylinder (4) through the pushrod (2); the pressure of the fluid increases and activates the brakes on the brake disk (5). (3) is the fluid reservoir. The hydraulic actuator is used to control the brake pedal position.

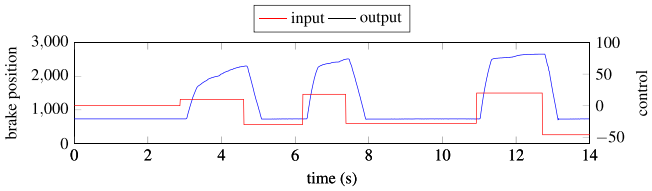

Fig. 5. Open-loop response of the brakes (experimental data).

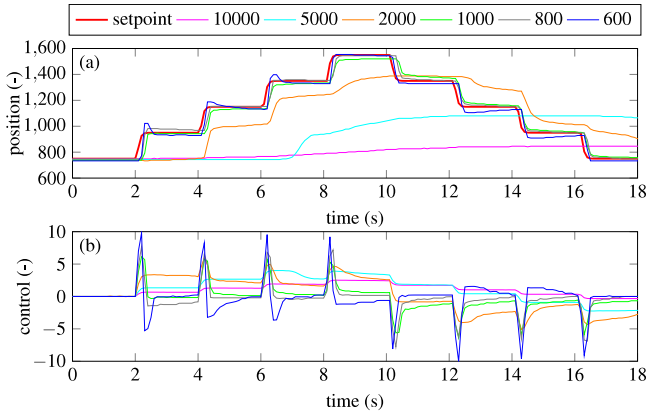

Fig. 6. Tuning of parameter α for the brake system. (For interpretation of the references to color in this figure legend, the reader is referred to the web version of this article.)

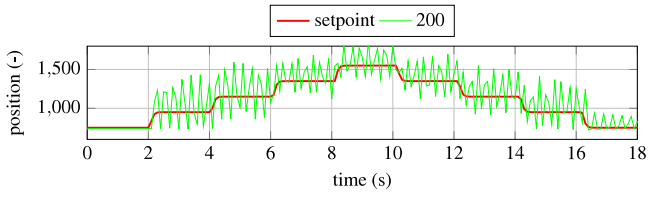

Fig. 7. Feedforward response for $\alpha = 200$ of the brake system.

of α (see Fig. 6), starting from $\alpha = 10000$ and decreasing its value until the output and the control signal starts to oscillate (at $\alpha = 200$, Fig. 7). Finally, the value of α is obtained : $\alpha = 800$. Then, the proportional gain K_P is increased such that the dynamics of the output error is acceptable, see Fig. 8. The final tuning of the i-P controller is then $\alpha = 800$, $K_P = 2 \times 10^{-3}$.

The obtained i-P controller is then compared to a PI controller using the same reference signal. The PI controller tuning is $K_P = 5 \times 10^{-2}$ and $K_I = 5 \times 10^{-3}$. The reference position of the brake pedal is shown in red in Fig. 9. The i-P controller performance is slightly better than the

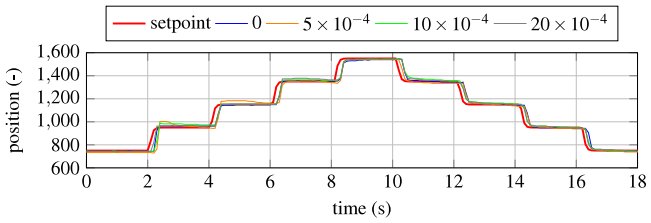

Fig. 8. Tuning of parameter K_P for the brake system. (For interpretation of the references to color in this figure legend, the reader is referred to the web version of this article.)

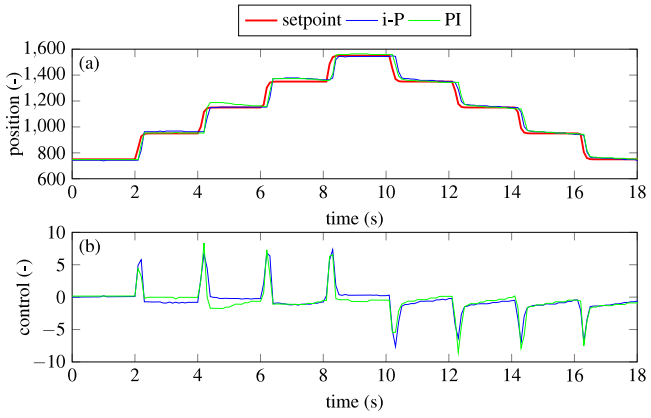

Fig. 9. Comparison between PI and i-P controllers for the brake system. (For interpretation of the references to color in this figure legend, the reader is referred to the web version of this article.)

PI one: it has been observed that it provides slightly lower steady-state error.

On a practical point of view, i-P controller has a simpler tuning procedure than the PI one. The α parameter is obtained in a systematic way. Then the K_P parameter is tuned empirically whereas for the PI, both parameters needs to be tuned at the same time.

In the rest of this work, the brake system will be controlled using the i-P controller with the parameter values obtained in this section.

4.2. Longitudinal speed control of the vehicle

In order to control the longitudinal speed of the vehicle, a model-free control approach is also used. The objective is to control the longitudinal speed of the vehicle y^v by computing u_v, the total wheel force requested. As depicted in Fig. 3, the actual total wheel force applied to the vehicle is subject to the dynamics of the low-level controllers. Although the velocity control is not highly challenging, it is still subject to the following difficulties: (i) at low speed, for small u_{ice}, as the GCU controls the vehicle velocity at 10 km/h using the clutch, the system is not controllable; (ii) during propelling, the system becomes non controllable when the clutch is open during a gear shift sequence; (iii) the low-level ICE torque is poorly controlled by the ECU and causes thus disturbances on the control signal.

Tests were performed on the track presented in Fig. 10. The track altitude profile is depicted in Fig. 11. The disturbance caused by the slope at the beginning of the track forces to use the brakes in order to maintain the vehicle at standstill.

In order to test the control law, the reference speed is composed of successive steps of ± 10 m/s triggered every 10 s. This raw reference signal is then smoothen using a second-order filter with time constant 0.4 s to obtain a C^1 speed reference, denoted y_r and shown in red in Figs. 12 to 15.

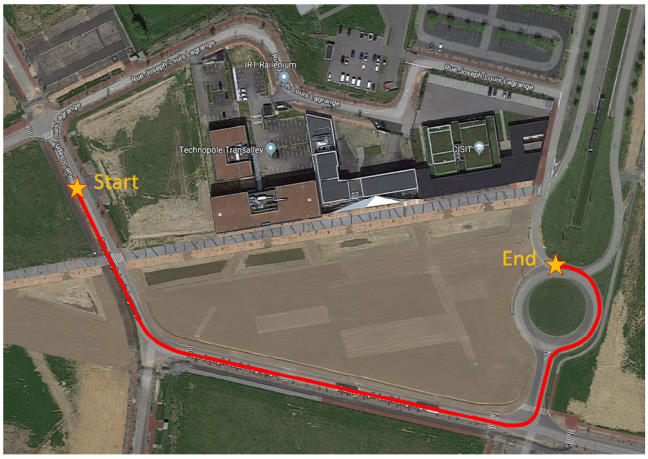

Fig. 10. Top view of the open road test field track.

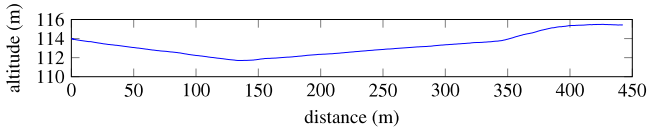

Fig. 11. Altitude of the track.

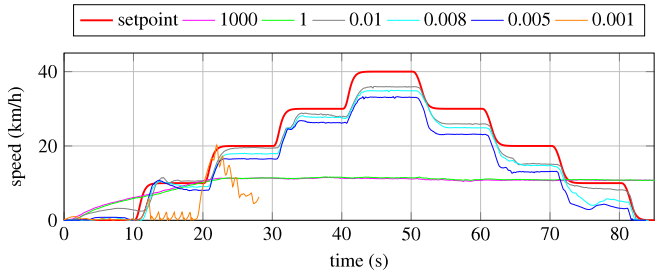

Fig. 12. Tuning of the α parameter for the high-level controller. (For interpretation of the references to color in this figure legend, the reader is referred to the web version of this article.)

4.2.1. Tuning of the control parameters

The procedure suggested in Section 3.2 has been applied for the tuning of α. Throughout this subsection, the time window of the ALIEN filter T is chosen equal to 0.1 s which is a good tradeoff between noise filtering and the filter bandwidth. The results obtained for different values of α using only the feedforward control law ($K_P = 0$) are shown in Fig. 12. For a better clarity, the absolute value of the tracking error e is displayed in Fig. 13.

For large α values such as $\alpha \in [1, 1000]$, the control amplitude is too low. In such situations, the gearbox control unit hands over the clutch and the engine to maintain the vehicle speed at approximatively 12 $\mathrm{km\,h^{-1}}$. This feature is standard for vehicle equipped with an automatic transmission. The reference tracking is improved by decreasing α. Acceptable values are between 0.005 and 0.01. As expected, when α is too low ($\alpha = 1 \times 10^{-3}$), the closed-loop becomes unstable and the experiment is stopped earlier for safety reasons. At this stage of the tuning procedure, $\alpha = 0.008$ is chosen.

The second part of the tuning procedure consists in choosing K_P such that the system output smoothly tracks the reference signal. If a perfect estimation for $\widehat{F}$ is assumed, then the closed-loop pole lay at $-\alpha K_P$ (see Eq. (8)). The closed-loop response should be perfectly damped. In practice, as shown in Fig. 14, it is not the case as some overshoots for large K_P can be observed. $K_P = 100$ is chosen as a trade-off between the closed-loop response time and overshoots.

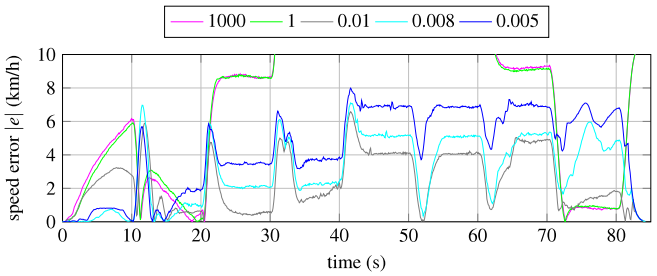

Fig. 13. Absolute value of the tracking error $e = y - y_r$ for different values of α ($K_P = 0$) for the high-level controller. (For interpretation of the references to color in this figure legend, the reader is referred to the web version of this article.)

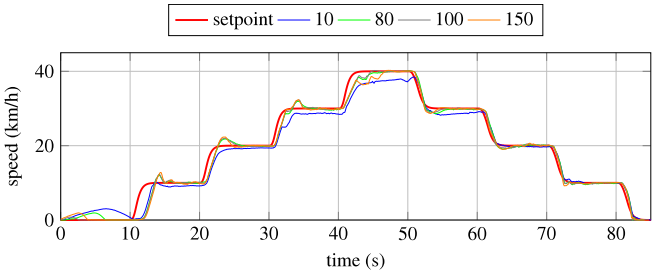

Fig. 14. Response of the model-free controller for different values of K_P and $\alpha = 0.008$. (For interpretation of the references to color in this figure legend, the reader is referred to the web version of this article.)

After a fine tuning of the parameters, the following final values are obtained for the i-P controller: $\alpha = 0.006$ and $K_P = 100$. The results are shown in blue in Fig. 15.

4.2.2. Comparison with a PI controller

Finally, the i-P controller is compared with a PI controller which is one of the most widespread controller. The main objective of this study being to propose a manual tuning of the controller, a similar approach has been used for the PI controller. Therefore, PID tuning methods have not been used even though there exists some model-free methods in the literature such as Iterative Feedback Tuning (Hjalmarsson et al., 1998), Direct Model Reference Adaptive Control (Pirabakaran & Becerra, 2001) and Virtual Reference Feedback Tuning (Formentin, Campi, & Savaresi, 2014). The PI controller has been hand-tuned to obtain a fast closed-loop response without too much overshoots over the chosen setpoint profile: the ICE engine should only be used to manage the accelerations whereas the deceleration phases could be manage using only the ICE engine brake and the mechanical brakes. The results are shown in Fig. 15. First, between $t \in [0, 10]$ s, both the i-P and the PI controllers are able to reject the disturbance due to the initial slope. Then, the i-P controller provides a faster tracking of the reference than the PI. This is due to the feedforward term $\dot{y}_r$ included in the control law, see Eq. (4). The PI controllers exhibits a 26% overshoots on the first step at $t = 15.2$ s. The i-P controller overshoot is only 7.8% at $t = 14.0$ s. Due to the system non-linearities, the other overshoots are smaller for both controllers. The overshoots of the PI controller can be reduced at the price of a slower tracking. Finally, the overall controller performances can be measured using the root mean square (RMS) of the tracking error. Data are given in Table 2. The i-P performs 36% better than the PI.

According to the authors' experience, the tuning of the PI controller was less intuitive than the i-P and did require more time and experimental trials. The system dynamics is strongly affected by the engaged gear. As the chosen PI controller has fixed gain, the final tuning has been chosen to average the performances over the gears 1 to 3 used in this experiment. Better tuning can be obtained on individual gears

Table 2
Comparison of the root mean square of the tracking error between PI and i-P controllers.

Controller	PI	i-P
RMSE (km/h)	2.32	1.48

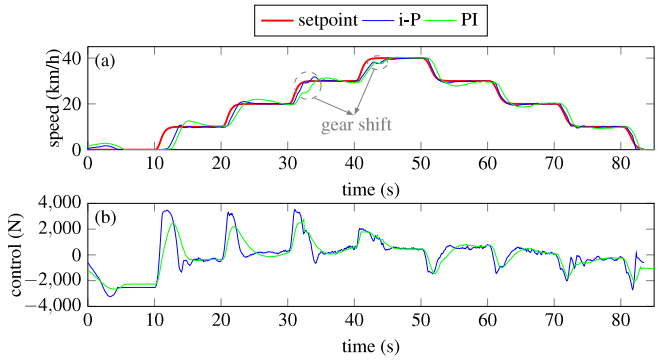

Fig. 15. Comparison of the speed profile between the i-P and PI controllers. (For interpretation of the references to color in this figure legend, the reader is referred to the web version of this article.)

at the price of worse performance on the other gears. On the contrary, the tuning of the i-P controller was relatively straightforward with the procedure proposed in Section 3.2. Moreover, it is less sensible to gear changes since the system dynamics is implicitly captured through the estimation of the unknown F.

During acceleration phases, gear shifts occur as shown in Fig. 15. They are engaged by the GCU whose control law is unknown. During this period, the clutch is opened. Therefore, the system is not controllable as the engine torque generated is not transmitted to the wheels. During deceleration phases, gear shifts happen too but do not impact the controllability of the system as the brakes can still be applied.

5. Conclusion and perspectives

This work discussed the design of model-free controllers based on ALIEN filters and their application on an actual vehicle. In particular, several important implementation details such as the required order for the numerical quadrature used to compute the ALIEN filters and the tuning of the control law parameters are presented. While the order of the numerical quadrature used to implement the ALIEN filter impacts the steady-state error, the tuning of the α parameter affects the transient behavior. Consequently, this paper provides general guidelines for an efficient implementation of model-free controllers. It has to be pointed out that this tuning procedure can be performed directly on the actual system without any prior simulations. Nevertheless, such a procedure should be followed with sufficient care as the order of magnitude of α and K_P are unknown in practice.

The MFC laws were used to control both the brake system and the longitudinal speed of an actual vehicle. The results illustrated the ability of this approach to control a system with unknown or complex dynamics. Due to the model-free feedforward action, the tuning becomes easier than for a classic PID.

Future works include a generalization of the tuning method to systems of any order ($\nu > 1$) and the development of a procedure to estimate the order ν when almost no information about the system is available. Moreover, more challenging applications such as the lateral control of an actual vehicle using model-free control are thought.

Declaration of competing interest

The authors declare that they have no known competing financial interests or personal relationships that could have appeared to influence the work reported in this paper.

Acknowledgments

The authors would like to thank the engineering school ENSIAME for enabling them to test algorithms on its autonomous vehicle. The present research was supported by the international research Chair MINES ParisTech - Peugeot-Citroen - Safran - Valeo on ground vehicle automation, the Regional Delegation for Research and Technology, the French Ministry of Higher Education and Research, and the National Center for Scientific Research. It was also supported by the ELSAT2020 project, co-funded by the European Regional Development Fund, the French state and the Hauts de France Region Council. The authors greatly acknowledge these institutions for their support.

Appendix A. Deriving the ultralocal model

Consider a system where y is the output and u the input. It can be written as an input–output differential equation in the form of Eq. (A.1) where $\mathcal{E}$ is a function not necessarily linear but assumed to be sufficiently smooth.

$$\mathcal{E}(t, y, \dot{y}, \dots, y^{(m)}, u, \dot{u}, \dots, u^{(n)}) = 0 \tag{A.1}$$

If there exist $\nu \in]0; m[$ such that $\frac{\partial \mathcal{E}}{\partial y^{(\nu)}} \neq 0$, the implicit function theorem yields then locally to:

$$y^{(\nu)} = \mathscr{E}(t, y, \dot{y}, \dots, y^{(\nu-1)}, y^{(\nu+1)}, \dots, y^{(m)}, u, \dot{u}, \dots, u^{(n)}) \tag{A.2}$$

In practice, ν is always equal to 1 or 2.

Appendix B. ALIEN filters

ALIEN filters were introduced in Fliess and Sira-Ramírez (2003). They are based on operational calculus (see Yoshida, 1984). In order to obtain Eq. (3), the following operations were made.

Starting from Eq. (1) with $\nu = 1$, assuming that F is a piecewise constant function, apply the Laplace transform:

$$sY(s) = \frac{F_s}{s} + \alpha U(s) + y(0) \tag{B.1}$$

Then, get rid of the initial condition $y(0)$ by multiplying by $\frac{d}{ds}$ on both sides. In order to obtain an equation only composed of terms in the form of Eqs. (B.2) and (B.3) for which the inverse Laplace transforms are known, multiply both side by s^{-2}. This leads to Eq. (B.4).

$$\frac{c}{s^\alpha}, \alpha \geq 1, c \in \mathbb{C} \Rightarrow c\frac{t^{\alpha-1}}{(\alpha-1)!}, t > 0 \tag{B.2}$$

$$\frac{1}{s^\alpha}\frac{d^n Y}{ds^n} \Rightarrow \frac{(-1)^n}{(\alpha-1)!}\int_0^T (T-\tau)^{\alpha-1}\tau^n y(\tau)\,\mathrm{d}\tau \tag{B.3}$$

$$\frac{Y(s)}{s^2} + \frac{1}{s}\frac{dY}{ds} = -\frac{F_s}{s^4} + \alpha\frac{1}{s^2}\frac{dU}{ds} \tag{B.4}$$

Applying Eqs. (B.2) and (B.3) to Eq. (B.4) leads to Eq. (3).

Appendix C. Stability proof for bounded estimation errors

Set $x_k = x(t_k) = x(kT_s)$ where x is a time-dependent variable and consider a discrete version of Eq. (7) with $\mathcal{K}(e) = K_P e$ (i-P controller). The derivative of the error at time k, denoted $\dot{e}_k$, is approximated by a forward Euler scheme: $\dot{e}_k = (e_{k+1} - e_k)/T_s$. The following equation on the error is thus obtained:

$$e_{k+1} = (1 - T_s\alpha K_P)e_k + T_s(F_k - \hat{F}_k) \tag{C.1}$$

Set $A = (1 - T_s\alpha K_P)$, $B = T_s$ and $f_k = (F_k - \hat{F}_k)$. Iterating from $t = 0$, one obtains (see Kermani, Delprat, Guerra, Trigui, & Jeanneret, 2012):

$$e_k = A^k e_0 + \sum_{i=0}^{k-1} A^i B f_{k-1-i} \tag{C.2}$$

Assume that the ∞-norm of the estimation error is bounded. In this case, $\forall k \in \mathbb{N}, |f_k| \leq f_{max} = |F - \widehat{F}|_{max}$. Thus, Eq. (C.2) becomes:

$$|e_k| \leq |A^k e_0| + \sum_{i=0}^{k-1} |A|^i |B| f_{max} = |A^k e_0| + (1 - |A|)^{-1}(1 - |A|^k)|B| f_{max} \quad \text{(C.3)}$$

If K_P and α are well chosen (*i.e.* $\frac{2}{T_s} > \alpha K_P > 0$), for sufficiently large k, $|A^k| \approx 0$, thus for any $\delta > 0$ sufficiently small (see Proof below for further details):

$$|e_k| \leq (1 + \delta) \left| \frac{1}{\alpha K_P} \right| |F - \widehat{F}|_{max} \quad \text{(C.4)}$$

Therefore, the system is stable as the tracking error e_k remains in a ball $\mathcal{B}\left(0, \left|\frac{f_{max}}{\alpha K_P}\right|\right)$ of radius $\frac{f_{max}}{\alpha K_P}$ centered in 0.

Proof. Let $\delta > 0$. Choosing K_P and α such that $|A| < 1$, i.e. $\frac{2}{T_s} \geq \alpha K_P \geq 0$, leads to $|A|^k \underset{k \to +\infty}{\longrightarrow} 0$.

Therefore,

$$\forall \epsilon > 0, \exists K \in \mathbb{N}^*, \forall k \in \mathbb{N}^*, k \geq K \Rightarrow |A|^k < \epsilon \quad \text{(C.5)}$$

Hence, Eq. (C.3) leads to:

$$\forall \epsilon > 0, \exists K \in \mathbb{N}^*, \forall k \geq K, |e_k| < \epsilon |e_0| + (1 + \epsilon) \left| \frac{f_{max}}{\alpha K_P} \right| \quad \text{(C.6)}$$

In particular, choosing $\epsilon = \frac{1}{\left(1 + |e_0| \left|\frac{\alpha K_P}{f_{max}}\right|\right)} \delta > 0$ which is defined as $f_{max} \neq 0$ leads to the presented results. Thus:

$$\forall \delta > 0, \exists K \in \mathbb{N}^*, \forall k \in \mathbb{N}^*, k \geq K, |e_k| \leq (1 + \delta) \left| \frac{1}{\alpha K_P} \right| f_{max} \quad \square \quad \text{(C.7)}$$

Appendix D. Numerical quadrature of ALIEN filters with trapezoidal rule

Eq. (3) is an analog equation which needs to be approximated numerically. A common approach used to discretize an integral is the *trapezoidal rule*. Define N as $N = \lfloor T/T_s \rfloor + 1$. Set $Y_k = y(t_k)$ and $U_k = u(t_k)$ with $t_k = kT_s$, for $k \in [\![0; N-1]\!]$. The trapezoidal rule applied to Eq. (3) gives:

$$-\frac{6}{T^3} \int_0^T [(T - 2\tau)y(\tau) + \alpha\tau(T - \tau)u(\tau)] \, \mathrm{d}\tau \approx \quad \text{(D.1)}$$
$$-\frac{6T_s}{T^3} \sum_{k=0}^{N-2} \left[(T - 2(k + \tfrac{1}{2})T_s) \left(\frac{Y_k + Y_{k+1}}{T_s} \right) \right]$$
$$-\frac{6T_s}{T^3} \sum_{k=0}^{N-2} \left[(k + \tfrac{1}{2})T_s (T - (k + \tfrac{1}{2})T_s) \left(\frac{\alpha_{k+1}U_{k+1} + \alpha_k U_k}{T_s} \right) \right]$$

At steady-state, $\dot{y} = 0$ and u is constant, thus $F_{exact} = -\alpha u$. The analog expression of the ALIEN filter given by Eq. (3) leads to:

$$\widehat{F}_{filter} = -\frac{6}{T^3} \int_0^T [(T - 2\tau)y + \tau(T - \tau)\alpha u] \, \mathrm{d}\tau = -\alpha u \quad \text{(D.2)}$$

However, the numerical quadrature of the integral using the trapezoidal rule leads to an estimation error $F - \widehat{F}$ at steady-state. More precisely:

$$\widehat{F}_{trap} = -\alpha u - \frac{1}{2} \left(\frac{T_s}{T} \right)^2 \alpha u \quad \text{(D.3)}$$

References

Åstrom, K. J., & Hägglund, T. (1995). *PID controllers: Theory, design, and tuning*. Instrument Society of America: Research Triangle Park.

Bara, O., Olama, M., Djouadi, S., Kuruganti, T., Fliess, M., & Join, C. (2017). Model-free load control for high penetration of solar photovoltaic generation. In *2017 North American power symposium (NAPS)*. Morgantown, United States.

Campi, M. C., Lecchini, A., & Savaresi, S. M. (2002). Virtual reference feedback tuning: a direct method for the design of feedback controllers. *Automatica*, *38*(8), 1337–1346.

Chand, A. N., Kawanishi, M., & Narikiyo, T. (2016). Non-linear model-free control of flapping wing flying robot using ipid. In *2016 IEEE international conference on robotics and automation (ICRA), Vol. 2016-June* (pp. 2930–2937). IEEE.

Choi, S., d'Andréa-Novel, B., Fliess, M., Mounier, H., & Villagra, J. (2009). *Model-free control of automotive engine and brake control for stop-and-go scenarios* (pp. 3622–3627).

Dahlquist, G., & Björck, Å. (2008). *Numerical methods in scientific computing, Volume I, Vol. 1* (pp. 1–13). Society for Industrial and Applied Mathematics.

d'Andréa-Novel, B. (2018). Model-free control of longitudinal and lateral dynamics for automated vehicles. *JTEKT Engineering Journal English Edition*, (1015), 1–7.

d'Andréa-Novel, B., Fliess, M., Join, C., Mounier, H., & Steux, B. (2010). A mathematical explanation via "intelligent" PID controllers of the strange ubiquity of PIDs. In *18th mediterranean conference on control and automation, MED'10* (pp. 395–400). IEEE.

d'Andréa-Novel, B., Menhour, L., Fliess, M., & Mounier, H. (2016). Some remarks on wheeled autonomous vehicles and the evolution of their control design. *IFAC-PapersOnLine*, *49*(15), 199–204.

Fliess, M., & Join, C. (2008). Intelligent PID controllers. In *2008 16th mediterranean conference on control and automation, Vol. 44* (pp. 326–331). IEEE.

Fliess, M., & Join, C. (2009). Model-free control and intelligent PID controllers: Towards a possible trivialization of nonlinear control?. *IFAC Proceedings Volumes*, *42*(10), 1531–1550.

Fliess, M., & Join, C. (2013). Model-free control. *International Journal of Control*, *86*(12), 2228–2252.

Fliess, M., & Sira-Ramírez, H. (2003). An algebraic framework for linear identification. *ESAIM. Control, Optimisation and Calculus of Variations*, *9*, 151–168.

Formentin, S., Campi, M. C., & Savaresi, S. M. (2014). Virtual reference feedback tuning for industrial PID controllers. *IFAC Proceedings Volumes*, *47*(3), 11275–11280.

Guardabassi, G. O., & Savaresi, S. M. (2000). Virtual reference direct design method: an off-line approach to data-based control system design. *IEEE Transactions on Automatic Control*, *45*(5), 954–959.

Hjalmarsson, H., Gevers, M., Gunnarsson, S., & Lequin, O. (1998). Iterative feedback tuning: theory and applications. *IEEE Control Systems Magazine*, *18*(4), 26–41.

Hou, Z., & Jin, S. (2013). *Model free adaptive control: theory and applications*. CRC press.

Hou, Z.-S., & Wang, Z. (2013). From model-based control to data-driven control: Survey, classification and perspective. *Information Sciences*, *235*, 3–35.

IFAC Industry Committee, 2015. Committee Conference Call, URL https://taskforce.ifac-control.org/industry-committee/legacy-materials-pilot-industry-committee-2014-2017/meeting-materials/meeting-presentation-17-june-2015/view (visited on 06.03.18).

Join, C., Chaxel, F., & Fliess, M. (2013). "Intelligent" controllers on cheap and small programmable devices. In *2013 conference on control and fault-tolerant systems (SysTol)* (pp. 554–559). IEEE.

Join, C., Masse, J., & Fliess, M. (2008). Etude préliminaire d'une commande sans modèle pour papillon de moteur. *Journal Europeen des Systemes Automatises*, *42*(2–3), 337–354.

Kermani, S., Delprat, S., Guerra, T., Trigui, R., & Jeanneret, B. (2012). Predictive energy management for hybrid vehicle. *Control Engineering Practice*, *20*(4), 408–420.

Menhour, L., d'Andréa-Novel, B., Fliess, M., Gruyer, D., & Mounier, H. (2015). A new model-free design for vehicle control and its validation through an advanced simulation platform. In *European control conference*. Linz, Austria.

Menhour, L., d'Andréa-Novel, B., Fliess, M., & Mounier, H. (2013). Multivariable decoupled longitudinal and lateral vehicle control: A model-free design. In *52nd IEEE conference on decision and control* (pp. 2834–2839). IEEE.

Milanés, V., Villagrá, J., Godoy, J., & González, C. (2012). Comparing Fuzzy and intelligent PI controllers in stop-and-go manoeuvres. *IEEE Transactions on Control Systems Technology*, *20*(3), 770–778.

Milanés, V., Villagrá, J., Perez, J., & González, C. (2012). Low-speed longitudinal controllers for mass-produced Cars: A comparative study. *IEEE Transactions on Industrial Electronics*, *59*(1), 620–628.

Miller, W., Werbos, P. J., & Sutton, R. S. (1995). *Neural networks for control*. MIT press.

Narendra, K. S., & Valavani, L. S. (1979). Direct and indirect model reference adaptive control. *Automatica*, *15*(6), 653–664.

Pirabakaran, K., & Becerra, V. M. (2001). Automatic tuning of PID controllers using model reference adaptive control techniques. In *IECON'01. 27th annual conference of the ieee industrial electronics society (Cat. No.37243), Vol. 1* (pp. 736–740 vol.1).

Schlömilch, O., Witzschel, B., Cantor, M., Kahl, E., Mehmke, R., & Runge, C. (1901). *Zeitschrift für mathematik und physik, Vol. 46*. B. G. Teubner.

Villagra, J., Milanes, V., Perez, J., & Gonzalez, C. (2010). Model-free control techniques for stop & go systems. In *Intelligent transportation systems (ITSC), 2010 13th international IEEE conference on* (pp. 1899–1904).

Wang, J., Mounier, H., Cela, A., & Niculescu, S. I. (2011). Event driven intelligent PID controllers with applications to motion control. *IFAC Proceedings Volumes (IFAC-PapersOnline), Vol. 18* (pp. 10080–10085). IFAC, URL http://dx.doi.org/103182/20110828-6-IT-100202960.

Yoshida, K. (1984). *Operational calculus, A theory of hyperfunction, Vol. 1*. Springer.

Zimmermann, H.-J. (1996). Fuzzy Control. In *Fuzzy set theory—and its applications* (pp. 203–240). Dordrecht: Springer Netherlands.